

# COMBINATION OF ATOMIC FORCE MICROSCOPY AND COMET ASSAY FOR ANALYSIS OF DNA DAMAGE INDUCED BY PDT

Hana Zapletalová<sup>1</sup>, Kateřina Bartoň Tománková<sup>1</sup>, Jakub Malohlava<sup>1</sup>,  
Milan Vůjtek<sup>2</sup>, Hana Kolářová<sup>1</sup>

<sup>1</sup>Department of Medical Biophysics, Institute of Molecular and Translational Medicine, Faculty of Medicine and Dentistry, Palacky University Olomouc, Czech Republic

<sup>2</sup>Department of Experimental Physics, Faculty of Science, Palacky University Olomouc, Czech Republic

## Abstract

The aim of the present study was to evaluate the efficiency of photosensitisation induced by two photosensitizers, TMPyP and ClAlPcS2, tested *in vitro* on the tumor cell line MCF7. The oxidative damage of DNA in MCF-7 cells was analyzed by comet assay (CA) combined with Atomic Force Microscopy (AFM). The ability of detection of apoptotic response detected by Atomic Force Microscopy at the individual molecule level of DNA was successfully demonstrated; when DNA get damaged, cleavage to fragments caused by photodynamic treatment was directly visualized by AFM imaging of individual molecules. Its accuracy and reliability was validated through the comparison with traditional single cell agarose electrophoresis.

## Keywords

photodynamic therapy, atomic force microscopy, DNA damage, comet assay

## Introduction

The atomic force microscopy (AFM) is the member of the scanning probe microscopes and since its invention in 1986 it has spread to the common practice in the different scientific disciplines. A wide range of samples were analyzed by AFM including both whole cells [1] tissues [2], but also the bacteria [3], the individual cell organelles, viruses [3, 4] or lipid layers and individual molecules [5]. In addition to the basic mode involving AFM applications in air, the AFM operates also in a vacuum or in liquids; popular function of AFM embraces a dynamic measurement of the sample in time. Apart from topographical information the AFM can collect data on the physical properties of the sample and provide 3D mapping of physical properties of the sample [6].

Atomic force microscopy (AFM) has been utilized for manipulating and imaging of individual DNA since 1989 [7–12]. AFM is one of the leading techniques in single molecule or nanoscale science because it can visualize individual DNA, proteins and DNA-protein complexes under physiological conditions in real time. However, AFM studies of DNA were mostly focused on the biological structure and dynamic processes of

DNA. Relatively limited application was developed in DNA damage and repair research [13–18].

As soon as the AFM was developed, the high effort has been done to visualize molecules like proteins and nucleic acids, either fixated or under physiological conditions. There are various methods used to detect DNA damage in single molecules [19, 20], also the AFM has shown good quantitative results. Some AFM studies used the interaction between repair proteins like glycosylases and damage recognition proteins and the damaged DNA to visualize the damage extend [13, 14]. Another approach is to image damaged plasmid molecules and determine the amount of super coiled plasmid vs. relaxed and linear plasmid, as DNA damage reduces the account of plasmids that are supercoiled [17, 18, 21].

Photodynamic therapy (PDT) is a minimally invasive therapeutic modality approved for treatment of cancer diseases and non-oncological disorders. This approach is based on local administration and the selective accumulation and retention of a photosensitizer in a tumor tissue followed by selective irradiation at the site of the tumor with light of the wavelength matching the absorption spectrum of the photosensitizer. The key role plays also the presence of oxygen in the treated

tissue and thus the local formation of reactive oxygen species [22].

After the exposure the photosensitizer to light of appropriate wavelength the absorption of photon occurs. The absorbed photon excites the photosensitizer to one or more energy-rich state(s). This can occur in one of two types of reactions: (a) the excited photosensitizer reacts directly with the substrate, in a one-electron transfer reaction, to produce a radical or a radical ion in both the sensitizer and the substrate. In the presence of oxygen, both radicals can further react to produce oxygenated products; (b) the excited photosensitizer transfers its excess energy to ground-state molecular oxygen ( $^3\text{O}_2$ ), producing excited state singlet oxygen ( $^1\text{O}_2$ ), and regenerating the ground-state sensitizer. Singlet oxygen then reacts with the substrate to generate oxidized products, subsequently oxidized lipids, amino acids and proteins and usually leads to cell death [23–25].

Photodynamic treatment activates series of cell signaling pathways and reactions inducing the stress, however the main objective of PDT is targeted cell death. What kind of processes leading to cell death will be activated after PDT affects the chemical structure and the concentration of PS in the irradiated tissue, the final location of the PS in the cell, the amount of available oxygen in the place of the action of the PS, the energy density (*exposure*, sometimes also referred to a *dose of radiation exposure*), the period between the PS uptake and light exposure and the type of the targeting tissue [24, 26–28]. The main goal of the optimization of PDT is therefore the choice of the appropriate PS according to the type of treated tissue and the final location of the PS in the cell, providing targeted transport to the malignant tissue in the organism and the setting up such a concentration of PS and values of light doses of radiation which leads to a marked preference of apoptotic processes from necrotic way of the cell death.

At molecular level, direct tumor cell destruction by PDT is caused by the irreversible photodamage to vital subcellular targets including the plasma membrane and intracellular membranes of the mitochondria, lysosomes, Golgi apparatus and endoplasmic reticulum. Since most photosensitizers do not accumulate in cell nuclei, PDT has generally a much lower potential of causing DNA damage, mutations and carcinogenesis as compared to X radiation at equitoxic doses [24]. Generally photoactive compounds localizing to the mitochondria or the endoplasmic reticulum promote apoptosis within a certain threshold of oxidative stress while PDT with photosensitizers targeting either the plasma membrane or lysosomes can either delay or block the apoptotic program predisposing the cells to necrosis [24, 29, 30].

Apoptotic process is an ATP requiring process characterized by chromatin condensation, cleavage of chromosomal DNA into internucleosomal fragments, cell shrinkage, membrane blebbing, formation of apoptotic

bodies without plasma membrane breakdown, exposure of phosphatidylserine in the outer leaflet of the plasma membrane and phagocytosis by neighboring cells. Apoptotic process is encoded in each mammalian cell and always includes the reversible signaling pathways and irreversible phase of signaling pathways induced by caspases, a family of proteases that have a cysteine at their active site. Once activated, caspases cleave, and thereby activate other procaspases (in particular, caspase-3, -6 and -7) resulting in an amplifying proteolytic cascade. Some of the activated caspases then cleave other key proteins in the cell. Some cleave the nuclear lamins, causing the irreversible breakdown of the nuclear lamina [31]; another cleaves a protein that normally holds a DNA-degrading enzyme (DNase) in an inactive form, freeing the DNase to cut up the DNA in the cell nucleus and are associated with a reduction of the kernel [27, 28, 32, 33].

The degradation of nuclear DNA into nucleosomal units is one of the best – characterized biochemical features and the hallmark of apoptotic cell death [34–39]. There are two phases of DNA digestion during apoptotic death. The first involves cleavage of the genome into 200–300 kbp and 30–50 kbp pieces through single strand breaks (SSBs), known a ‘domain’ cleavage causing release of the quaternary structure of DNA. This phase is triggered by apoptosis inducing factor (AIF) released from mitochondria [32, 33]. The second phase involves further cleavage of DNA producing oligonucleosomal fragments of the typical length of 180–200 bp and multiples (so-called CAD-dependent DNA fragmentation) [40].

DNA isolated from cytotoxic (genotoxic in particular) damaged cells typically has clearly reduced the degree of winding due to the emergence of SSBs. While double strand breaks (DSBs) occur, DNA fragmentation may be evident. Arising from the fragments, or the length distribution of fragments, one can directly visualize the level of the fragmentation electrophoretically or by AFM, in case of AFM the fragmentation of the individual molecules [41, 42].

Necrosis is morphologically characterized by vacuolization of the cytoplasm, swelling and breakdown of the plasma membrane resulting in an inflammatory reaction due to release of the cellular content. Necrosis is thought to be the end result of a bio-energetic catastrophe resulting from ATP depletion to a level incompatible with cell survival [22, 28].

The phototoxic effect of PDT can be assessed by single cell electrophoresis – a comet assay (CA). The comet assay is a simple, sensitive and quantitative technique for the detection of DNA damage at the level of individual cells. Analyzed cells are embedded in agarose, lysed, and electrophoresed at high pH. DNA, being negatively charged, is drawn towards the anode during electrophoresis. A strand break relaxes supercoiling of DNA, and so broken loops are able to extend towards the anode, and it is these loops that form the comet tail (Fig. 1). The head consists of intact DNA

while the tail is created from broken fragments of DNA and relaxed chromatin. The relative size of the tail (most conveniently measured as the % of total fluorescence in the tail or head) reflects the number of DNA loops and therefore the frequency of DNA breaks [43–45].

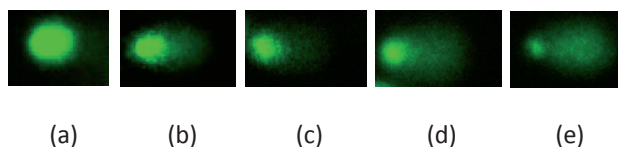


*Fig. 1: Typical comet images of MCF7 cells treated with TMPyP and light irradiation, representing different levels of DNA damage: (a) undamaged DNA (comet without tail); (b-d) levels of DNA damage; (e) the most damaged DNA.*

## Material and methods

### Cell line and culture conditions

The human breast cancer MCF-7 cell line was cultured in DMEM medium supplemented with 10% fetal calf serum and antibiotics (streptomycin (0,1 g/l), penicillin (0,1 g/l)) and L-glutaimn (0,3 g/l) and incubated in thermo-box at 37 °C and 5% CO<sub>2</sub> in 96-well plates or 35 mm culture plates.

The MCF7 cells were incubated with TMPyP (0 μM as a control, 1 μM, 5 μM, 50 μM) or CIAIPcS<sub>2</sub> (0 μM as a control, 0,1 μM, 0,5 μM, 10 μM) for 24 h and in the dark of the thermo-box prior to light irradiation. Prior to photoirradiation of cells the dye-containing medium was replaced with PBS. The second group of control cells (50 μM TMPyP and 10 μM CIAIPcS<sub>2</sub>) were incubated in the thermo-box with experimental cell groups until tripsynization. Five experimental groups ((1) control cells with variable concentration of photosensitizer without irradiation, (2) cells without photosensitizer irradiated with light only and three cell groups treated with different photosensitizer concentrations and fixed irradiation dose) were tested in triplicate. 50 μM TMPyP and 10 μM CIAIPcS<sub>2</sub> concentrations of the PS and light dose were chosen according to the IC<sub>50</sub> that yielded 50% cell viability according to MTT test.

### Chemicals and reagents

The chemicals used were Dulebecoo's modified Eagle's medium (DMEM), phosphate buffered saline (PBS, pH 7.4), TMPyP meso-tetra (4-N-methylpyridyl) porphyrin and CIAIPcS<sub>2</sub> (Sigma-Aldrich), dimethyl sulfoxide (DMSO, Sigma-Aldrich), HMP agarose (Serva), LMP agarose (Qbiogene), trypsin-ethylenediaminetetraacetic acid (EDTA, Sigma), ethanol (Sigma), fetal bovine serum (FBS, Sigma-Aldrich),

NaCl (Tamda), EDTA (Lachema), tris [tris(hydroxymethyl) aminomethane, Sigma-Aldrich], Triton X-100 (Serva), NaOH (Sigma-Aldrich), SYBR®Green (Invitrogen), , kit for genomic DNA isolation (Qiagen).

### The instrument

Fuorescent microscope Olympus IX81 with DSU unit (Olympus), centrifugal machine (Biotech), electrophoretic tank (Bio-RAD, Nano-drop (FisherSci) and atomic force microscope Bioscope Catalyst (Bruker) were used. Acquired data were proceeded using Comet Score freeware 1.5 (Tritek Corp, Sumerduck, VA, USA), Nanoscope analysis (Bruker, Santa Barbara, CA, USA).

### Sensitization of cells

MCF7 cells treated with TMPyP and CIAIPcS<sub>2</sub> (except control cells) were sensitized by a home-made LED based light source especially designed for the irradiation of experimental microplates. The emitters of a wavelength of 414 nm (10 mW/cm<sup>2</sup>), radiation dose 1 J/cm<sup>2</sup> for TMPyP treated cells and 660 nm (10 mW/cm<sup>2</sup>), radiation dose 5 J/cm<sup>2</sup> for CIAIPcS<sub>2</sub> treated cells were used. Irradiation was carried out at room temperature, followed by incubation of the culture in the dark in the thermo-box for 4 h or 6 h. At different time points following PDT (4 hours and 6 hours), cells were collected from the monolayer with trypsin and washed 2times with PBS. All assays were performed in triplicate.

### Comet assay

The comet assay determines the percentage of DNA damage. We used the protocol from our previous study [46]. Briefly, microscope glass slides were first precoated with 1% HMP agarose. The treated cells were trypsinized, rinsed with DMEM with 10% FBS, and centrifuged (6 minutes, 1,000 rpm). A volume of 85 μL of 1% LMP agarose was added to cell suspension and 85 μL of this mixture was put on the microscope slide coated with agarose gel. The microscope slides were immersed in a lysis buffer for 1 hour, placed in an electrophoretic tank and dipped into a electrophoresis solution (7 °C) for 40 minutes. Electrophoresis was run at 0.8 V/cm and 380 mA for 20 minutes. After neutralization in a buffer (0.4 M Tris, pH = 7.5), the samples were stained with SYBR® Green and immediately examined with a fluorescent microscope (Olympus IX81) and scored using SW Comet Score. The values of DNA head percentage, tail length and olive tail moment were selected for assessment of DNA damage.

### DNA isolation and immobilization

PDT treated MCF-7 cells and non-treated control MCF-7 cells were harvested by tripsinization and

washed 2times with PBS. DNA was isolated by standard kit for genomic DNA isolation (NORGEN BIOTEK). Aliquots of DNA (5 µg/ml in 40 mM HEPES, 10 mM MgCl<sub>2</sub>, pH 7,6) were kept at -20 °C or used immediately to AFM imaging. APS-mica was used for the binding of DNA molecules. APS-mica was prepared as described by [47]. A drop of 5 µl of DNA solution (DNA concentration of 0.5–1.0 µg/ml) was deposited on the APS mica surface at room temperature for 3 min. The sample was rinsed and dried before imaging.

### Atomic force microscopy and data analysis

AFM imaging was performed in air using atomic force microscopy tip ScanAsyst Air with resonant frequency 45–95 kHz, spring constant 0.2–0.8 N/m with tip radius 2 nm. Scan rate was set at 0.3 Hz. AFM surface images were acquired in a tapping mode at the scan resolution of 512x512 pixels and scan sizes of 1000–5000 nm. Image data processing (slope correction and flattening) were done by NANOSCOPE software 8.

The measurement of the length of DNA fragments adsorbed on mica surface has been processed by image analysis (OLYMPUS IX81 software).

## Results and discussion

### Comet assay

Nuclear DNA is organized in tertiary structure in nucleosomal units in living cells. Supercoiled DNA is thus firmly anchored in agarose gel and the shape of the comets form the core of the cell. The basic factor determining whether a segment of DNA in the tail of the comet appears rather than in the head, is the relaxation of the winding supercoiled DNA. The relaxation of supercoiled DNA depends on the single and double strand breaks. DNA fragments (bearing negatively charged surface) then migrate to the anode and create a specific tail, the image of the comet, which corresponds to the frequency of the breaks in the thread of DNA, therefore the number of unwind loops of DNA. With increasing degree of damage increases the intensity of the tail of a comet than its length. The amount of DNA in the tail of the comet then reflects the nature of the damage – the concentration of substances examined or the irradiation dose.

The cytotoxic effect of two photosensitizers (TMPyP and ClAlPcS<sub>2</sub>) was studied using different photosensitizer concentrations at fixed dose of radiation (1 J/cm<sup>2</sup> and 5 J/cm<sup>2</sup>). The treatment induced by 50 µM TMPyP and 1 J/cm<sup>2</sup> for MCF7 cells and 10 µM ClAlPcS<sub>2</sub> and 5 J/cm<sup>2</sup> for MCF7 corresponds to IC<sub>50</sub> (MTT test), data not showed. The samples exposed to the radiation dose of 0 J/cm<sup>2</sup> exhibit no degree of the DNA fragmentation and correspond to the majority content of DNA in the head (Fig. 2 and Fig. 3).

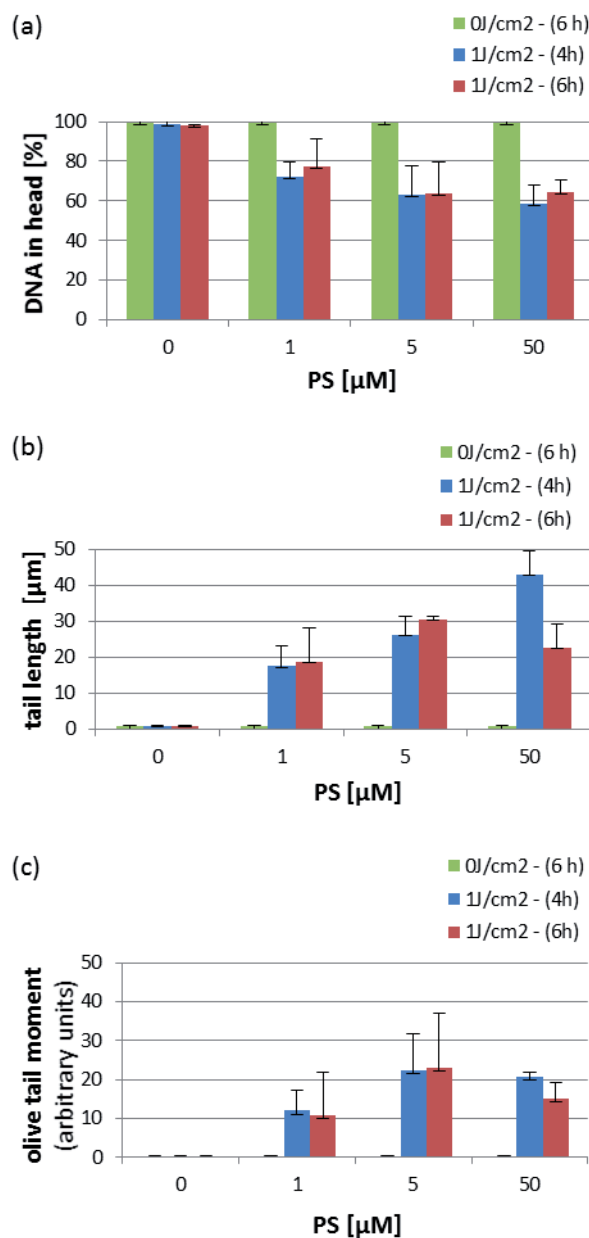


Fig. 2: Comet assay of TMPyP treated cells. Results are expressed as (a) percentage DNA in head, (b) tail length, (c) olive tail moment. Green columns represent control cells with maximum photosensitizer concentration without light irradiation – control (50 µM TMPyP, 0 J/cm<sup>2</sup>), blue columns represent results obtained 4 hours after PDT, red columns represent results obtained 6 hours after PDT.

The Fig. 2 shows that 10 times higher concentration of TMPyP (5 µM and 50 µM of TMPyP, respectively) at 1 J/cm<sup>2</sup> light dose causes comparable DNA damage, 4 hours after irradiation: (63±14) % DNA in head and (59±9) % DNA in head respectively; 6 hours after irradiation: (63±16) % DNA in head and (64±6) % DNA in head respectively. This apparent regression or even decrease in DNA damage in spite of

the increase level of the cell damage induction is caused by the saturation of the comet assay [44].

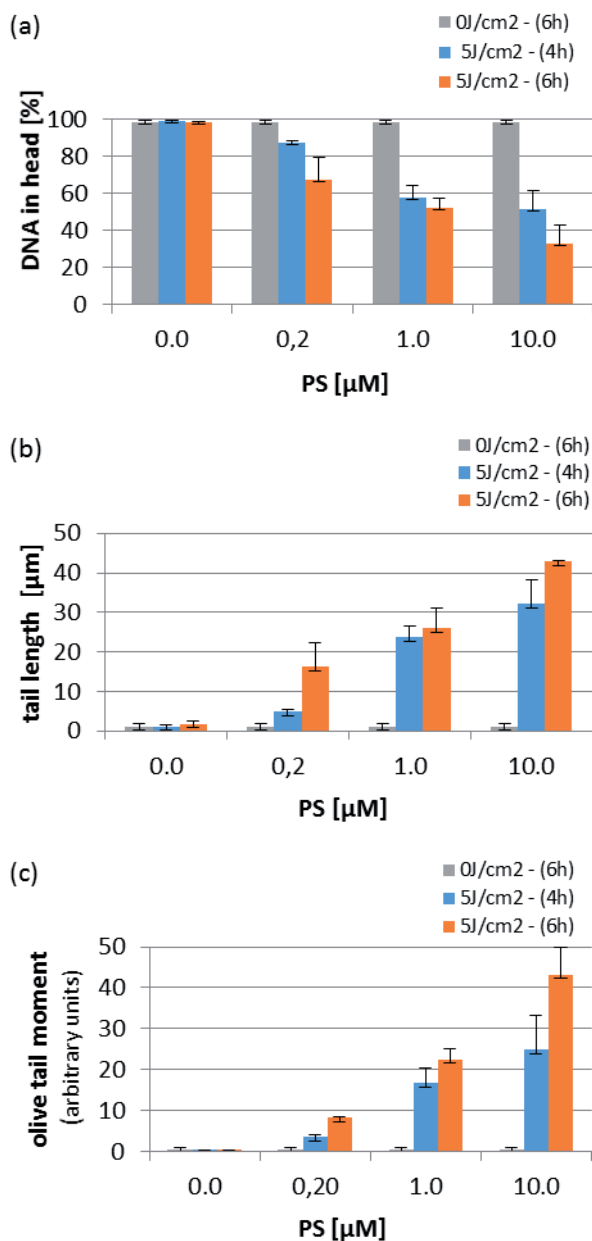


Fig. 3: Comet assay of CIAIPcS<sub>2</sub> treated cell. Results are expressed as (a) percentage DNA in head, (b) tail length, (c) olive tail moment. Green columns represent control cells with maximum photosensitizer concentration without light irradiation – control (10 μM CIAIPcS<sub>2</sub>, 0 J/cm<sup>2</sup>), blue columns represent results obtained 4 hours after PDT, red columns represent results obtained 6 hours after PDT.

The similar result shows also Fig. 3, comparing results of 1 μM CIAIPcS<sub>2</sub> and 10 μM CIAIPcS<sub>2</sub>: 4 hours after irradiation: (58±4) % DNA in head and (51±6) % DNA in head respectively; 6 hours after irradiation: (51±9) % DNA in head and (32±8) % DNA in head respectively.

We can conclude that the saturation of comet assay was reached at 10times lower concentration of photosensitizer (TMPyP either CIAIPcS<sub>2</sub>) compared to value of IC<sub>50</sub>, whether in the earlier stage – 4 h after irradiation or in stage 6 h after irradiation.

By comparing the time period after PDT we can assume the induction of repair processes (Fig. 2) at low concentration level of TMPyP (1 μM TMPyP and 1 J/cm<sup>2</sup>), since the amount of DNA in head is higher 6 hours after PDT treatment (77±14) % DNA in head compared to 4 hours (72±7) % DNA in head.

On the contrary CIAIPcS<sub>2</sub> at low concentration level (0.5 μM CIAIPcS<sub>2</sub> and 5 J/cm<sup>2</sup>) indicates the growth of DNA damage at 6 hours after PDT treatment (67±12) % DNA in head compared to 4 hour interval: (87±2) % DNA in head.

The results of comet assay revealed that both TMPyP and CIAIPcS<sub>2</sub> are cytotoxic at low concentrations levels (1 μM TMPyP, 0.5 μM CIAIPcS<sub>2</sub>) and low light dose (1 J/cm<sup>2</sup> and 5 J/cm<sup>2</sup> respectively).

Furthermore, TMPyP has higher toxicity in comparison with CIAIPcS<sub>2</sub>, comparing to the concentration of the photosensitizers and the irradiation dose equivalent to IC<sub>50</sub>.

#### Atomic force microscopy

AFM scans of control samples (0 μM TMPyP and 1 J/cm<sup>2</sup>; 0 μM CIAIPcS<sub>2</sub> and 5 J/cm<sup>2</sup>; 50 μM TMPyP and 0 J/cm<sup>2</sup>; 10 μM CIAIPcS<sub>2</sub> and 0 J/cm<sup>2</sup>) clearly showed supercoiled DNA molecules with DNA length of thousands base pairs (bp).

Also, AFM images of DNA isolated from PDT treated cells almost always showed the similar structure – long twisted fibers that could not identify length of individual strains (Fig. 4b, Fig. 5b).

Only the lowest concentration of TMPyP (1 μM TMPyP) and low light dose (1 J/cm<sup>2</sup>) induced clear fine DNA fragmentation in MCF-7 cells (Fig. 4a, Fig. 6). However, these fragments are not presented in the image of DNA isolated from cells treated with higher concentration of TMPyP.

MCF7 cells treated by PDT induced by CIAIPcS<sub>2</sub> and light dose (5 J/cm<sup>2</sup>) show low level of DNA fragmentation after treatment with 0,5 μM CIAIPcS<sub>2</sub>, as there was found presence of short DNA fragments in the AFM images (Fig. 5a). However, these fragments are not presented in the image of DNA isolated from cells treated with higher concentration of identical PS (1 μM CIAIPcS<sub>2</sub>, 10 μM CIAIPcS<sub>2</sub>).

Image analysis of fragmented DNA (Fig. 6) shows cleavage of chromatin DNA into nucleosomal fragments of roughly 180 bp/~60 nm and multiples thereof (360 bp/~122 nm, 540 bp/~183 nm etc.), induced by 1 μM TMPyP, light dose 1 J/cm<sup>2</sup>. The shortest DNA fragments (180 bp/~60 nm and shorter) are tightly packed and visualized mainly as globular shape whereas longer fragments (360 bp/~120 nm and longer) take a linear form.

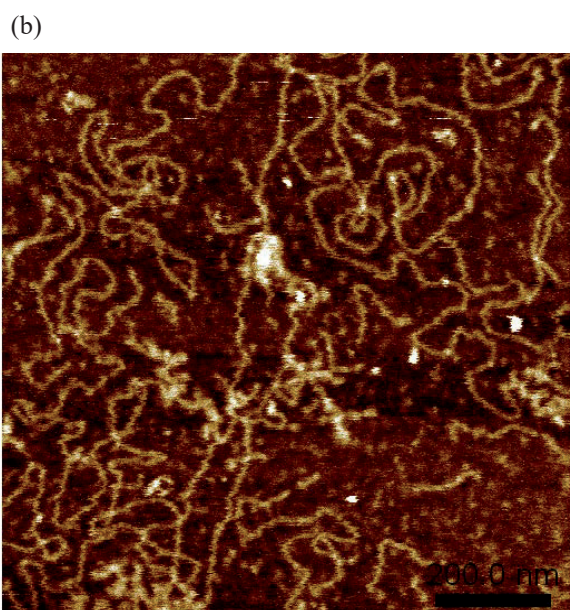
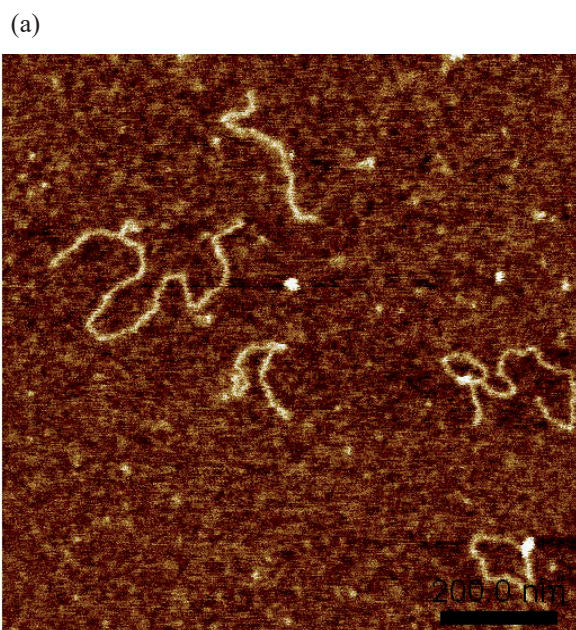


*Fig. 4: Representative AFM images of DNA isolated from MCF-7 cells treated by TMPyP and  $1 \text{ J/cm}^2$ . tapping mode, scan rate  $0,2 \text{ Hz}$ , (a)  $1 \mu\text{M}$  TMPyP,  $1 \text{ J/cm}^2$  (b)  $50 \mu\text{M}$  TMPyP,  $1 \text{ J/cm}^2$ , scan size  $1 \times 1 \mu\text{m}^2$ .*

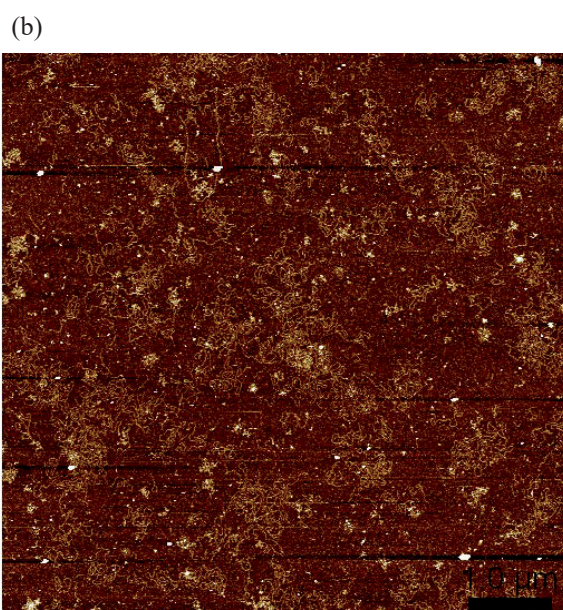
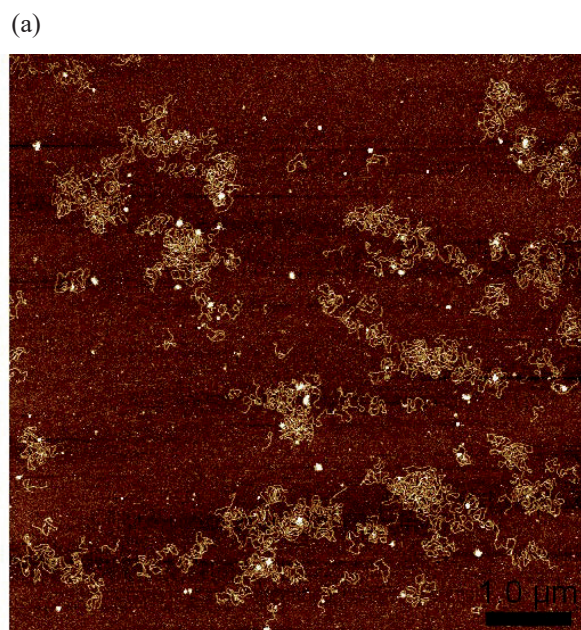


*Fig. 5: Representative AFM images of DNA isolated from MCF-7 cells treated by ClAlPcS<sub>2</sub> and  $5 \text{ J/cm}^2$ , tapping mode, scan rate  $0,2 \text{ Hz}$ , scan size  $5 \times 5 \mu\text{m}^2$ . (a)  $0,5 \mu\text{M}$  ClAlPcS<sub>2</sub>,  $5 \text{ J/cm}^2$  (b)  $10 \mu\text{M}$  ClAlPcS<sub>2</sub>,  $5 \text{ J/cm}^2$ .*

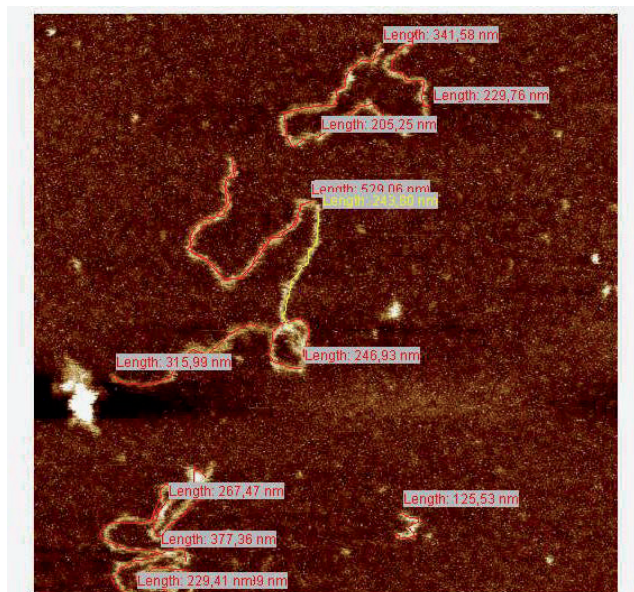


Fig. 6: Image analysis of AFM image of DNA isolated from MCF-7 cells treated by  $1 \mu\text{M}$  TMPyP,  $1 \text{ J/cm}^2$ , scan size  $1 \times 1 \mu\text{m}^2$ .

## Conclusion

The methods compared in this study provide an effective evaluating of DNA damage induced by cytotoxic agents – in our case photodynamic treatment. The comet assay has a well-deserved popularity. It is simple and economical method detecting DNA damage in a “physiological range” – e.g. at levels that are found in living cells treated with moderate doses of damaging agent.

Comet analysis confirmed that both studied sensitizers are significantly cytotoxic even at small concentrations of photosensitizers and the radiation dose. The results of comet assay proved that TMPyP sensitizer is more efficient photosensitizer compared to CIAIPcS<sub>2</sub> as could be found in [48].

In addition, AFM method revealed a hint of apoptotic processes – a fine DNA fragmentation ( $1 \mu\text{M}$  TMPyP,  $1 \text{ J/cm}^2$ ). In the second sensitizer, CIAIPcS<sub>2</sub> fine fragmentation phenomenon was observed with much lower occurrence on the AFM images ( $0.5 \mu\text{M}$  CIAIPcS<sub>2</sub>).

This finding is probably related to the different mechanism of action of both sensitizers. Prior to irradiation TMPyP is localized mainly in lysosomes and delocalizes into the nucleus and nucleoli after irradiation [49] and bind directly to the DNA [50] causing DNA cleavage due to ROS production [51, 52].

In contrast the localization of CIAIPcS<sub>2</sub> is primarily in the mitochondria and the cytotoxic effect of PDT is executed through damage of mitochondrial membrane [53].

Different from the traditional techniques, the second damage detection method based on AFM imaging is performed at a single-molecule level with higher sensitivity and consumes less DNA materials than bulk methods. Based on our AFM results we showed that AFM is a potential tool for DNA damage examination on single molecule level.

## Acknowledgement

The authors gratefully acknowledge the support provided by project LO1304 of the Ministry of Education, Youth and Sports of the Czech Republic, and IGA\_LF\_2016\_013.

## References

- [1] Tomankova, K., Kolarova, H., Bajgar, R., et al. Study of the photodynamic effect on the A549 cell line by atomic force microscopy and the influence of green tea extract on the production of reactive oxygen species. *Ann N Y Acad Sci* 2009, 1171: 549–558.
- [2] Antunes, A. GFV. Atomic Force Imaging of Ocular Tissues: morphological study of healthy and cataract lenses. *Modern Research and Educational Topics in Microscopy*, 2007 <http://www.formatex.org/microscopy3/pdf/pp29-36.pdf> (2007, accessed 10 May 2016).
- [3] Doktycz, M.J., Sullivan, C.J., Hoyt, P.R., et al. AFM imaging of bacteria in liquid media immobilized on gelatin coated mica surfaces. *Ultramicroscopy* 2003, 97: 209–216.
- [4] Kuznetsov, Y.G., McPherson, A.: Atomic Force Microscopy in Imaging of Viruses and Virus-Infected Cells. *Microbiol Mol Biol Rev* 2011, 75: 268–285.
- [5] S. Kasas NHT. Biological applications of the AFM: From single molecules to organs. *International Journal of Imaging Systems and Technology* 1997, 8: 151–161.
- [6] Casuso, I., Rico, F., Scheuring, S.: Biological AFM: where we come from--where we are--where we may go. *J Mol Recognit* 2011, 24: 406–413.
- [7] Hansma, H.G., Vesenska, J., Siegerist, C., et al. Reproducible imaging and dissection of plasmid DNA under liquid with the atomic force microscope. *Science* 1992, 256: 1180–1184.
- [8] Lyubchenko, Y.L.: DNA structure and dynamics: An atomic force microscopy study. *Cell biochemistry and biophysics* 2004, 41: 75–98.
- [9] Weisenhorn, A.L., Gaub, H.E., Hansma, H.G., et al. Imaging single-stranded DNA, antigen-antibody reaction and polymerized Langmuir-Blodgett films with an atomic force microscope. *Scanning Microsc* 1990, 4: 511–516.
- [10] Bustamante, C., Keller, D., Yang, G.: Scanning force microscopy of nucleic acids and nucleoprotein assemblies. *Current Opinion in Structural Biology* 1993, 3: 363–372.
- [11] Mou, J., Czajkowsky, D.M., Zhang, Y., et al. High-resolution atomic-force microscopy of DNA: the pitch of the double helix. *FEBS Letters* 1995, 371: 279–282.
- [12] Kasas, S., Thomson, N.H., Smith, B.L., et al. Escherichia coli RNA polymerase activity observed using atomic force microscopy. *Biochemistry* 1997, 36: 461–468.
- [13] Chen, L., Haushalter, K.A., Lieber, C.M., et al. Direct visualization of a DNA glycosylase searching for damage. *Chem Biol* 2002, 9: 345–350.
- [14] Wang, H., Yang, Y., Schofield, M.J., et al. DNA bending and unbending by MutS govern mismatch recognition and specificity. *Proc Natl Acad Sci USA* 2003, 100: 14822–14827.

- [15] Psonka, K., Brons S, Heiss M, et al. Induction of DNA damage by heavy ions measured by atomic force microscopy. *J Phys: Condens Matter* 2005, 17: S1443.
- [16] Murakami, M., Hirokawa, H., Hayata, I.: Analysis of radiation damage of DNA by atomic force microscopy in comparison with agarose gel electrophoresis studies. *Journal of Biochemical and Biophysical Methods* 2000, 44: 31–40.
- [17] Jiang, Y., Ke, C., Mieczkowski, P.A., et al. Detecting Ultraviolet Damage in Single DNA Molecules by Atomic Force Microscopy. *Biophysical Journal* 2007, 93: 1758–1767.
- [18] Ke, Ch., JY, Mieczkowski, P.A., Muramoto, P.A., et al. Nanoscale Detection of Ionizing Radiation Damage to DNA by Atomic Force Microscopy. *Small* 2008, 4: 288–294.
- [19] Filippova, E.M., Monteleone, D.C., Trunk, J.G., et al. Quantifying double-strand breaks and clustered damages in DNA by single-molecule laser fluorescence sizing. *Biophys J* 2003, 84: 1281–1290.
- [20] Flusberg, B.A., Webster, D.R., Lee, J.H., et al. Direct detection of DNA methylation during single-molecule, real-time sequencing. *Nat Methods* 2010, 7: 461–465.
- [21] Jiang, Y., Rabbi, M., Kim, M., et al. UVA Generates Pyrimidine Dimers in DNA Directly. *Biophysical Journal* 2009, 96: 1151–1158.
- [22] Buytaert, E., Dewaele, M., Agostinis, P.: Molecular effectors of multiple cell death pathways initiated by photodynamic therapy. *Biochim Biophys Acta* 2007, 1776: 86–107.
- [23] Allison, R.R., Moghissi, K.: Photodynamic Therapy (PDT): PDT Mechanisms. *Clin Endosc* 2013, 46: 24–29.
- [24] Oleinick, N.L., Morris, R.L., Belichenko, I.: The role of apoptosis in response to photodynamic therapy: what, where, why, and how. *Photochem Photobiol Sci* 2002, 1: 1–21.
- [25] Triesscheijn, M., Baas, P., Schellens, J.H.M.: et al. Photodynamic therapy in oncology. *Oncologist* 2006, 11: 1034–1044.
- [26] Mroz, P., Yaroslavsky, A., Kharkwal, G.B., et al. Cell Death Pathways in Photodynamic Therapy of Cancer. *Cancers* 2011, 3: 2516–2539.
- [27] Roos, W.P., Kaina, B.: DNA damage-induced cell death by apoptosis. *Trends in Molecular Medicine* 2006, 12: 440–450.
- [28] Castano, A.P., Demidova, T.N., Hamblin, M.R.: Mechanisms in photodynamic therapy: part two—cellular signaling, cell metabolism and modes of cell death. *Photodiagnosis and Photodynamic Therapy* 2005, 2: 1–23.
- [29] Kessel, D., Oleinick, N.L.: Initiation of autophagy by photodynamic therapy. *Meth Enzymol* 2009, 453: 1–16.
- [30] Kessel David: Subcellular Localization of Photosensitizing Agents. *Photochemistry and Photobiology* 1997, 387–388.
- [31] Kramer, A., Liashkovich, I., Oberleithner, H., et al. Caspase-9-dependent decrease of nuclear pore channel hydrophobicity is accompanied by nuclear envelope leakiness. *Nanomedicine* 2010, 6: 605–611.
- [32] Mc Gee, M.M., Hyland, E., Campiani, G., et al. Caspase-3 is not essential for DNA fragmentation in MCF-7 cells during apoptosis induced by the pyrrolo-1,5-benzoxazepine, PBOX-6. *FEBS Letters* 2002, 515: 66–70.
- [33] Vittar, N.B.R., Awruch, J., Azizuddin, K., et al. Caspase-independent apoptosis, in human MCF-7c3 breast cancer cells, following photodynamic therapy, with a novel water-soluble phthalocyanine. *The International Journal of Biochemistry & Cell Biology* 2010, 42: 1123–1131.
- [34] Bortner, C.D., Oldenburg, N.B.E., Cidlowski, J.A.: The role of DNA fragmentation in apoptosis. *Trends in Cell Biology* 1995, 5: 21–26.
- [35] Nagata, S., Nagase, H., Kawane, K., et al. Degradation of chromosomal DNA during apoptosis. *Cell Death Differ* 2003, 10: 108–116.
- [36] Nagata, S.: Apoptotic DNA Fragmentation. *Experimental Cell Research* 2000, 256: 12–18.
- [37] Semenov, D.V., Aronov, P.A., Kuligina, E.V.: et al. Oligonucleosome DNA fragmentation of caspase 3 deficient MCF-7 cells in palmitate-induced apoptosis. *Nucleosides Nucleotides Nucleic Acids* 2004, 23: 831–836.
- [38] Janine D Miller EDB. Photodynamic therapy with the phthalocyanine photosensitizer Pc 4: The Case experience with pre-clinical mechanistic and early clinical-translational studies. *Toxicology and applied pharmacology* 2007, 224: 290–9.
- [39] Kolarova, H., Macecek, J., Nevrelva, P., et al. Photodynamic therapy with zinc-tetra(p-sulfophenyl)porphyrin bound to cyclodextrin induces single strand breaks of cellular DNA in G361 melanoma cells. *Toxicology in Vitro* 2005, 19: 971–974.
- [40] Earnshaw, W. C.: Nuclear changes in apoptosis. *Curr Biol* 1995, 337–343.
- [41] Jiang, Y., Rabbi, M., Mieczkowski, P.A., et al. Separating DNA with Different Topologies by Atomic Force Microscopy in Comparison with Gel Electrophoresis. *J Phys Chem B* 2010, 114: 12162–12165.
- [42] Tiner Sr, W.J., Potaman, V.N., Sinden, R.R., et al. The structure of intramolecular triplex DNA: atomic force microscopy study. *Journal of Molecular Biology* 2001, 314: 353–357.
- [43] Collins, A.R.: Measuring oxidative damage to DNA and its repair with the comet assay. *Biochimica et Biophysica Acta (BBA) - General Subjects* 2014, 1840: 794–800.
- [44] Collins, A.R.: The comet assay for DNA damage and repair. *Mol Biotechnol* 2004, 26: 249–261.
- [45] Shaposhnikov, S., Brunborg, G., Azqueta, A., et al. Novel formats for the comet assay. *Toxicology Letters* 2013, 221, Supplement: S189.
- [46] Tomankova, K., Kejlova, K., Binder, S., et al. In vitro cytotoxicity and phototoxicity study of cosmetics colorants. *Toxicol In Vitro* 2011, 25: 1242–1250.
- [47] Zapletalová, H., Přibyl, J., Vůjtek, M., et al. Improved Method for Surface Immobilization of DNA Molecules Used in AFM Single Molecule Imaging. *Journal of Colloid and Interface Science*, 2016.
- [48] Pizova, K., Bajgar, R., Fillerova, R., et al. C-MYC and C-FOS expression changes and cellular aspects of the photodynamic reaction with photosensitizers TMPyP and CIAIPcS2. *J Photochem Photobiol B, Biol* 2015, 142: 186–196.
- [49] Patito, I.A., Rothmann, C., Malik, Z.: Nuclear transport of photosensitizers during photosensitization and oxidative stress. *Biol Cell* 2001, 93: 285–291.
- [50] Saeko Tada-Oikawa SO: DNA Damage and Apoptosis Induced by Photosensitization of 5, 10, 15, 20-Tetrakis(N -methyl-4-pyridyl)-21 H, 23 H -porphyrin via Singlet Oxygen Generation. *Photochemistry and photobiology* 2009, 85: 1391–9.
- [51] Bruce Armitage: Photocleavage of Nucleic Acids. 1998 1998, 98: 1171–1200.
- [52] Mettath, S., Munson, B.R., Pandey, R.K.: DNA interaction and photocleavage properties of porphyrins containing cationic substituents at the peripheral position. *Bioconjug Chem* 1999, 10: 94–102.
- [53] El-Hussein, A., Harith, M., Abrahamse, H.: Assessment of DNA Damage after Photodynamic Therapy Using a Metall-o-phthalocyanine Photosensitizer. *International Journal of Photoenergy* 2012, 2012: 281068.

Mgr. Hana Zapletalová  
Ústav lékařské biofyziky, Lékařská fakulta  
Univerzita Palackého v Olomouci  
Hněvotínská 3, CZ-775 15 Olomouc  
E-mail: hana.zapletalova@upol.cz  
Tel.: +420 585 632 111

Mgr. Milan Vůjtek, Ph.D.  
Katedra experimentální fyziky, Přírodovědecká fakulta  
Univerzita Palackého v Olomouci  
17. listopadu 1192/12, CZ-775 15 Olomouc